

# 1 Intensity calibration including pile-up effect in PHA 2 spectra measurements at W7-X

---

3 **M. Kubkowska<sup>a</sup>, M. Gruca<sup>a</sup>, S. Jabłoński<sup>a</sup>, L. Ryc<sup>a</sup>, U. Neuner<sup>b</sup> and the W7-X team**

4 <sup>a</sup> *Institute of Plasma Physics and Laser Microfusion,*  
5 *Hery 23, 01-497 Warsaw, Poland*

6 <sup>b</sup> *Max Planck Institute for Plasma Physics,*  
7 *17491 Greifswald, Germany*

8 *E-mail: [monika.kubkowska@ifpilm.pl](mailto:monika.kubkowska@ifpilm.pl)*

9 **ABSTRACT:** The pulse-height-analysis (PHA) is a technique used at fusion devices for  
10 measurements of content and intensity of the X-ray spectrum. At the stellarator W7-X, this  
11 method is applied together with the application of silicon drift detectors for observation of the  
12 radiation in the energy range from about 0.5 to 20 keV [1-2]. To receive quantitative information  
13 on plasma impurity concentration, several factors should be taken into account. Firstly, the  
14 detector response curve which includes the transmission of filters and detector thickness. In this  
15 case, the response was determined from the knowledge of the detector's geometry and  
16 characteristics of materials used, as calibration measurements with a standard X-ray radiation  
17 source were not possible. Secondly, the geometry parameters which define the observation cone  
18 of view, and finally, the pile-up effect which is a crucial point in intensity calibration. The pile-  
19 up effect can be minimized by settings of the lower values of the digital filter peaking time in X-  
20 ray signal processor (DXP), but often it is a compromise between energy resolution and temporal  
21 resolution of the time-dependent X-ray intensity signal. The information about the number of lost  
22 photons can be derived from the knowledge of the number of photons incoming to the detector  
23 and the number of photons observed in a spectrum. For the PHA system dedicated to W7-X, the  
24 loss of the pulses which undergo pileup is determined by values of the parameters: input count  
25 rate - ICR and output count rate – OCR, both delivered by the DXP. It is always taken into account  
26 in the intensity spectra calibration which allows to study the changes in impurity line intensity  
27 and hence to determine the impurity concentration.

28 **KEYWORDS:** X-ray detectors, nuclear instruments and methods for hot plasma diagnostics, data  
29 processing methods.

---

30	<b>Contents</b>	
31	<b>1. Introduction</b>	<b>1</b>
32	<b>2. Detectors and accompanying electronics</b>	<b>2</b>
33	<b>3. Calibration of the spectra</b>	<b>3</b>
34	3.1. Calculation of the pile-up effect	4
35	3.2. Removal of the pile-up events in DXP	5
36	<b>4. Summary</b>	<b>5</b>
37		
38		
39		

---

## 40 1. Introduction

41 The control of the amount and distribution of impurities in magnetically confined plasmas is one  
 42 of the big challenges in a magnetic fusion research, in particular, in the research based on  
 43 stellarator concept, which can relatively easily be operated continuously [1]. Understanding of  
 44 the transport characteristic of the impurities in stellarator plasmas is crucially important. For this  
 45 purpose, the proper operation of the diagnostics is significant [2-3].

46 The stellarator Wendelstein 7-X (W7-X) is the largest and the most advanced type of fusion  
 47 devices in the world aimed to demonstrate steady-state plasma operation [4].

48 One of the diagnostics installed on W7-X, dedicated for observation of soft X-ray radiation  
 49 in broad energy range, is the pulse-height-analysis system (PHA) [5-6]. This spectrometer  
 50 consists of 3 channels equipped with Silicon Drift Detectors (SDDs) and Beryllium foils of  
 51 various thicknesses, which allow the observation of spectra from about 0.5 to 20 keV. The  
 52 detectors are placed at the distance of 8 m from the plasma centre and in the line of sight of each  
 53 detector, a pinhole consisting of two piezo-slits is located. The change of aperture provides the  
 54 possibility of regulation of incoming photon flux (input count rate, ICR). It should be noticed that  
 55 with changing the pinhole size, the volume of plasma changes as well. For the largest aperture,  
 56 1.2 mm, the PHA system observes 35 mm in the plasma centre.

57 The electronics associated with detectors consists of a preamplifier and a multichannel  
 58 Digital X-ray signal Processor (DXP), in which analogue signals are amplified, digitized, filtered  
 59 by the use of digital filter (to obtain high signal to noise ratio), processed to remove pile-up, and  
 60 then routed to a histogramming memory. The DXP needs adjusting (by changing its parameters)  
 61 to each type of the detector and the preamplifier.

62 As the physical processes in the stellarator plasma are very fast, the acquisition time of a  
 63 spectrum must be set possibly short to reveal the detailed time structure of the measured signals.  
 64 In case of the PHA system, the time is set in the range of 50-100 ms, depending on the plasma  
 65 conditions. At such a short acquisition time, the PHA system must operate at a possibly high  
 66 counting rate to obtain reasonable good counting statistics, and on the other hand, to observe  
 67 spectra with a good energy resolution. In performed W7-X experiments, the FWHM is not worse  
 68 than 200 eV at the counting rate up to 600 kHz.

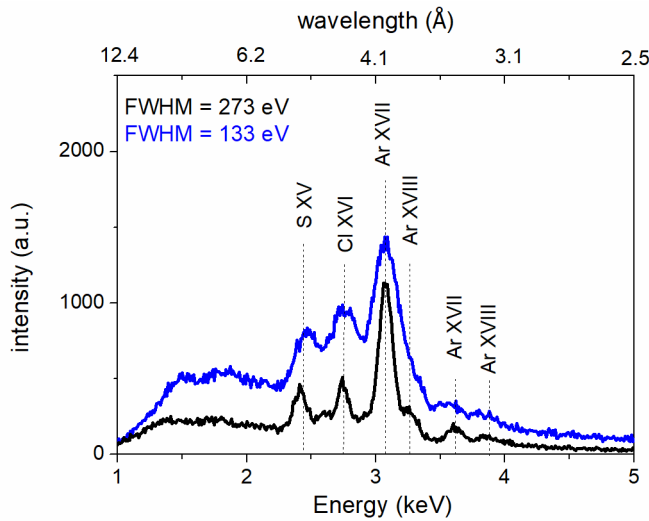
69 **2. Detectors and accompanying electronics**

70 In the PHA system dedicated to W7-X, Silicon Drift Detectors (SDD) from PNDetector are  
71 applied [7]. In two of three channels, SDDs of round shape and surface area of 10mm<sup>2</sup> (SDD-10-  
72 130 BeWic), covered by 8-um of Be are installed, while in the third channel, SDD with the same  
73 surface area but droplet design and filtered by a thin Polymer window (SDD-10-128pnW  
74 UTWic), is used. The detectors are equipped with an integrated Field-Effect Transistor (FET)  
75 and both elements are cooled. Peltier coolers coupled with the detector chip are responsible for  
76 the cooling up to -15°C which reduces the dark current and improves the energy resolution of  
77 collected spectra.

78 The detector converts each photon into photoelectron which later produces a cloud of  
79 electron-hole pairs. Thanks to the applied field gradient, the electrons and holes are then drifted  
80 towards electrodes. The accumulated charge is converted to a voltage signal by the FET  
81 preamplifier. The produced charge is proportional to the energy carried by incoming photons. The  
82 signal from the preamplifier is digitized in A/D converter at the input of the pulse processor while  
83 the digital filtering is responsible for shaping and noise reduction. The preamplifier is connected  
84 to the digital pulse processor (DPP) and data acquisition electronics. The PHA system works in  
85 the multi-channel analyzer (MCA) mode. The spectrum from each detector is measured usually  
86 in 1024 energy channels with the MCA bin width set to 10 - 30 eV.

87 There are several parameters which must be set by the operator in the acquisition software for the  
88 PHA spectra collection. Besides the MCA channel number and bin width which in combination  
89 with chosen thickness of Be filter define the observed energy range, the value of peaking time  
90 must be also specified. This parameter, which is related to the number of points which are  
91 averaged by the digital filter, can be set in the range from 0.1 up to 164 μs. For longer values,  
92 better energy resolution can be obtained but at the cost of increased dead time and thus lower  
93 output count rate (OCR) (worse statistics). To increase data throughput as much as possible, the  
94 peaking time during the first W7-X campaign (OP1) was set to 1μs which allowed for observation  
95 of the PHA spectra with resolution sufficient to resolve spectral lines. Fig. 1 presents an example  
96 of collected spectra for two chosen peaking times, for 0.3 μs and for 1 μs. It is clearly seen that  
97 for lower peaking time value (0.3μs) resolution is worse than the one for higher peaking time (1  
98 μs) which prevents resolving Ar XVII and Ar XVIII lines. Table 1 presents the list of spectral  
99 lines presented in fig.1 with corresponding wavelength and transitions. It should be noted that  
100 only dominant lines have been identified.

101  
102



103  
104 Fig. 1. Example PHA spectra collected for peaking time equal to 1  $\mu$ s (—) and 0.3  $\mu$ s (—).  
105

106 Table 1. Identified spectral lines presented in fig.1 with corresponding wavelength and transitions.

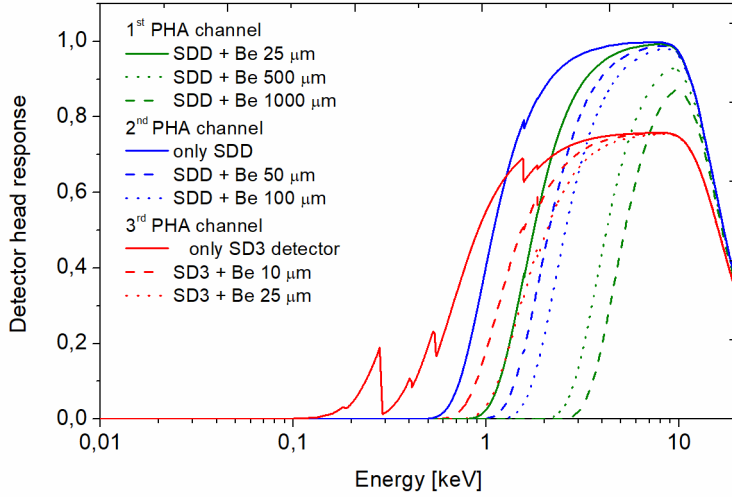
Type of line	Energy (eV)	Wavelength ( $\text{\AA}$ )	Transition
He-like S ( $S^{+14}$ )	2460.6255	5.038	$(1s2p)^1P_1 \rightarrow (1s^2)^1S_0$
He-like Cl ( $Cl^{+15}$ )	2789.808	4.444	$(1s2p)^1P_1 \rightarrow (1s^2)^1S_0$
He-like Ar ( $Ar^{+16}$ )	3139.5515	3.949	$(1s2p)^1P_1 \rightarrow (1s^2)^1S_0$
H-like Ar ( $Ar^{+17}$ )	3321.4	3.731	$(2p)^2P_{3/2} \rightarrow (1s)^2S_{1/2}$
He-like Ar ( $Ar^{+16}$ )	3683.8429	3.365	$(1s3p)^1P_1 \rightarrow (1s^2)^1S_0$
H-like Ar ( $Ar^{+17}$ )	3935.3	3.150	$(3p)^2P_{3/2} \rightarrow (1s)^2S_{1/2}$

107  
108 The second also important parameter is a trigger threshold which is responsible for the low-energy  
109 limit for the fast filter, which is used primarily for pileup inspection. Depending on the PHA  
110 energy channel, it was set to 1000 eV for the 1<sup>st</sup> and 2<sup>nd</sup> energy channel, and 360 eV for the low  
111 energy channel.

### 112 3. Calibration of the spectra

113 The PHA system at the W7-X has a dedicated for energy calibration port which is equipped with  
114 the mini X-ray tube. The radiation of this lamp excite the spectra of elements located inside the  
115 PHA port (stainless steel and Cu plates). Thanks to the observed fluorescence spectra and later,  
116 identification of well-known spectral lines, it is possible to complete the energy calibration curve  
117 [8]. To perform the intensity spectra calibration, an X-ray source of known intensity is needed.  
118 The precise calibration of the efficiency of detectors themselves is performed on the synchrotron  
119 Bessy [9], lately with the use of an absolute cryogenic thermal detector [10], but in case of the  
120 PHA system dedicated to W7-X, it was not possible to calibrate the whole spectrometer (including  
121 electronics) this way. Also, a calibrated X-ray lamp or a standard radioactive source of intensity  
122 high enough, which would simulate plasma emission were not used as they were not available.  
123 Instead of direct calibration, self-calibration [11] of detectors and filters is performed based on  
124 known material characteristics and geometrical parameter. The detectors response curves have  
125 been calculated based on the transmission of the Be window (with additional 30-nm Aluminum

126 on the detector surface) and additional filters, as well as absorption of the active detector depth  
 127 (450- $\mu\text{m}$  of Si) [12]. Figure 2 presents the detector response curves of each of the PHA channel  
 128 including extra Be filters.



129  
 130 Fig. 2. Detector response curves for each of the PHA channels with accompanying filters.  
 131

132 To calculate the measured spectra emissivity  $\varepsilon$  ( $\text{W}\cdot\text{eV}^{-1}\cdot\text{m}^{-3}$ ), geometrical factor is needed to  
 133 be known. This parameter depends on the pinhole size, distance between plasma-pinhole and  
 134 detector surface  $S_D$ . It is defined as:

$$135 \quad A = \frac{4\pi}{\sum_i S_D \cdot \cos(\alpha_i) \cdot \Delta V_i / R_i^2} \quad (1)$$

136 where  $\alpha$  is an angle between the connecting line for each plasma point  $i$  and the vector  
 137 perpendicular to the detector surface  $S_D$ ,  $R_i$  is the distance between plasma and detector surface,  
 138 while  $\Delta V_i$  is a volume of the plasma element  $i$ . The detailed description can be found in [8].

139 The second important parameter which must be taken into account is the pile-up effect which  
 140 always creates losses in the observed number of photons.

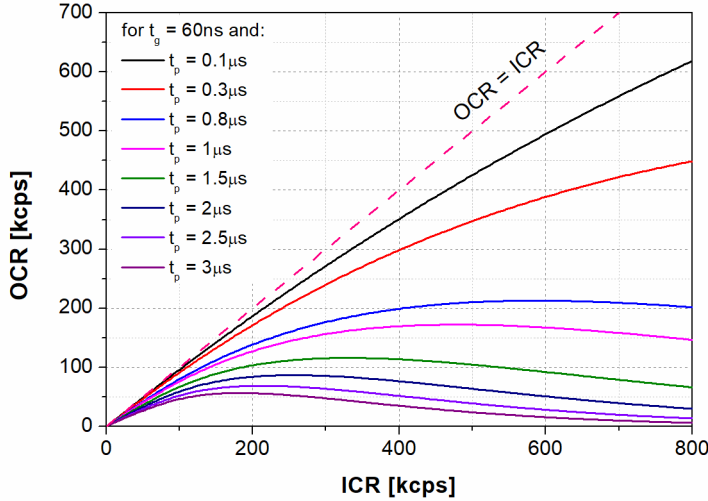
### 141 3.1. Calculation of the pile-up effect

142 The measured spectrum will only be a valid measure of number of photons and their associated  
 143 X-ray energy provided that the filtered pulse is sufficiently well separated in time from its  
 144 preceding and succeeding neighbor pulses so that its peak amplitude is not distorted by  
 145 overlapping. In the case of overlapping, one deals with the pile-up effect, which manifests itself  
 146 in production of multiple amplitude peaks in addition to the main peak. In the spectrometers based  
 147 on the digital techniques (with digital filters) all pile-up peaks are removed, but due to the process  
 148 of cleaning, some input pulses are lost from the final statistics. Output count rate (OCR) of pulses  
 149 is then always lower than the input count rate (ICR) of X-ray quanta interacting in the SDD  
 150 detector according to statistical formula (2) [13]. Assuming that dead time  $\tau_d$  for the slow channel  
 151 of the measuring system is known, one can apply the following formula to calculate the real ICR,  
 152 which refers to OCR:

$$153 \quad \text{OCR} = \text{ICR}_r \times \exp(-\text{ICR}_r \cdot \tau_d) \quad (2)$$

154 In the case of the DXP Mercury-4 from XIA [14] used in the PHA spectrometer for W7-X,  
 155 for the first approximation,  $\tau_d$  is expressed by  $2(t_p + t_g)$ , where  $t_p$  and  $t_g$  are the parameters of the  
 156 trapezoidal digital filter known as peaking time and gap time, correspondingly. The  $t_p$  is rising

157 and falling time, and the  $t_g$  duration of the flat top of the filter. The gap  $t_g$  is introduced to remove  
 158 the effect of fluctuation in rise time of output pulses, which arise from the irregularity of charge  
 159 collection in a detector and as a result improves energy resolution. The gap should be optimized  
 160 to obtain the highest energy resolution. The relations OCR – ICR for different values of peaking  
 161 time  $t_p$  are shown in fig. 3.



162  
 163 Fig.3. Theoretical curves of incident count rate (ICR) and output count rate (OCR) for various  
 164 peaking times,  $t_p$ .

165  
 166 The DXP Mercury-4 delivers the value of input count rate taken from the output of fast  
 167 channel, but it is somewhat lower than the real frequency of coming quanta because fast channel  
 168 has its own dead time  $\tau_{df}$ . To obtain the real input count rate  $ICR_r$  of quanta having measured input  
 169 count rate from the fast channel ( $ICM_m$ ) the following formula is used:

$$170 \quad ICM_m = ICR_r \times \exp(-ICR_r \cdot \tau_{df}) \quad (3)$$

171 The equation (2) should be inverted to obtain  $ICR_r$ .

172 Usually, during the last W7-X experimental campaigns, the pile-up effect was oscillating in the  
 173 range from 15% to 35 % depending on plasma conditions and pinhole size (photon flux).

### 174 3.2. Removal of the pile-up events in DXP

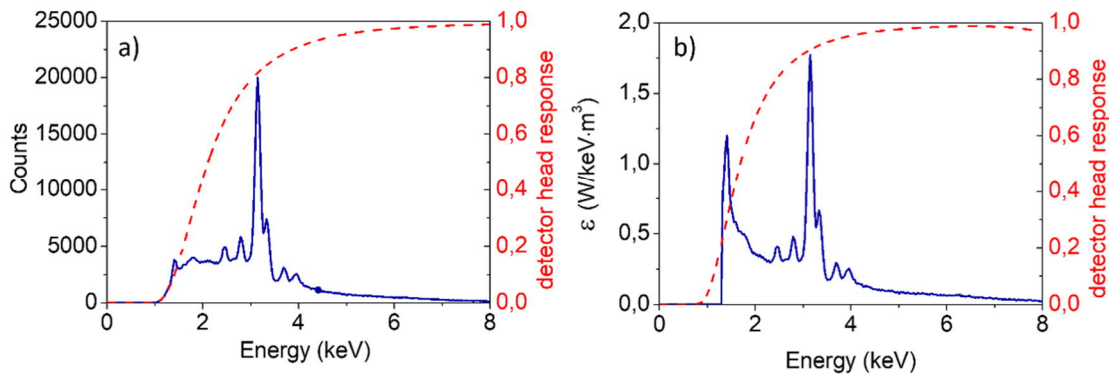
175 Two parallel processings of signals from incident photons are applied in the PHA system based  
 176 on Mercury-4, one in the fast channel which is used especially for the pile-up inspection and the  
 177 second one in the slow channel which is used for determination of amplitude of pulses. Such  
 178 separation of both functions is especially useful in the case of a strong photon flux.

179 There are two tests for inspection of pile-up events, both performed in the fast channel. The  
 180 first test is based on measuring the distance between two subsequent (triangular) pulses in the fast  
 181 channel. They must be separated far enough to avoid the pile-up in the slow channel and the  
 182 distance is related to the peaking time of the slow channel. The pile-up in the slow channel occurs  
 183 always when pulses are so close that the rising (or falling) edge of one pulse lies under the peak  
 184 of its neighbor pulse. Overlapped pulses in the slow channel are then removed.

185 The second test is based on measuring the width of pulses in the fast channel. If a pulse is  
 186 found to exceed certain fixed value (related to the peaking time of the fast channel), the fast -  
 187 channel pile-up takes place, and it leads to pile-up in the slow channel as well. The corresponding  
 188 cluster of pulses in the slow channel, which is of abnormally high amplitude, is then removed.

#### 189 4. Summary

190 The PHA spectra can deliver information about the kind of impurities in the W7-X plasma but  
191 only calibrated one can reveal information about the physical processes like impurity transport.  
192 Typical PHA spectrum, measured during the W7-X campaign, is presented in fig. 4a. Around  
193 1.2keV increase of radiation is visible, which results from the applied filter (50 $\mu$ m of Be), for  
194 which the transmission rapidly increases from 1 keV. For the same reason, the sharp increase in  
195 calibrated spectra (fig. 4b) is observed.



196  
197 Fig.4. Example of measured PHA spectrum (a) and corresponding calibrated spectrum (b)  
198 including filter transmission and pile-up losses. The spectrum was collected by the 2<sup>nd</sup> PHA  
199 channel with 50 $\mu$ m of Be filter.

200

201 It is clearly visible that calibrated spectrum (fig. 4b) exhibits different features than the measured  
202 one. The change in the shape of the spectrum is determined by the transmission of the filter and  
203 absorption of the detector. The correction for pile-up is made by multiplication of the spectrum  
204 by a constant value determined with reference to the theoretical curve presented in Fig. 3, which  
205 shows relation between input and output count rate and according to the formula (3). Additionally,  
206 the geometrical factor is also included in the calibration process according to the equation (1).  
207 The part of the spectrum below about 1.5 keV is not reliable because of high error in determination  
208 of transmission efficiency, which is smaller than 5%.

209 Proper calibration of the PHA spectra enables to deliver qualitative and quantitative  
210 information regarding radiation from the W7-X plasmas for different impurities. Determination  
211 of line intensities allows to estimate contribution of each impurity with respect to average plasma  
212 density and, in consequence, predict the plasma evolution and better understand the possible  
213 radiation collapse, due to both intrinsic and external impurities.

214 Moreover, the proposed method of PHA spectra calibration allows the cross-calibration with  
215 other diagnostic like XICS spectrometer (X-ray imaging crystal spectrometer) which delivers  
216 plasma flow profiles by measuring the Doppler shift of X-ray line emission from various  
217 impurities [15-16].

#### 218 Acknowledgments

219 This scientific paper has been published as part of the international project called 'PMW', co-  
220 financed by the Polish Ministry of Science and Higher Education within the framework of the  
221 scientific financial resources for 2021.

222 This work has been carried out within the framework of the EUROfusion Consortium and has  
223 received funding from the Euratom research and training programme 2014-2018 and 2019-2020  
224 under grant agreement No 633053. The views and opinions expressed herein do not necessarily  
225 reflect those of the European Commission.

## 226 **References**

- 227 [1] A. H. Boozer 1998 PoP **5** 1647
- 228 [2] M. Kubkowska et al. 2018 Problems of Atomic Science and Technology **6(118)** 312
- 229 [3] A. Langenberg et al. 2019 Plasma Phys. Control. Fusion **61** 014030
- 230 [4] T. Klinger et al. 2017 Plasma Phys. Control. Fusion **59** 014018
- 231 [5] N. Krawczyk et al. 2017 Fus. Eng. Des. **123** 1006
- 232 [6] M. Kubkowska et al. 2018 Fus. Eng. Des. **136** 58
- 233 [7] PNDetector Homepage, 2014 – 2021, Products & Applications, <https://pndetector.de/>
- 234 [8] M. Kubkowska et al. 2018 Rev. Sci. Instrum. **89** 10F111
- 235 [9] F. Scholze et al 2006 Microchim. Acta 155, 275–278
- 236 [10] M. Gerlach et al. 2008 Metrologia 45 577
- 237 [11] M. Krumrey et al 1992 Rev,Sci. Instrum. 63, 797
- 238 [12] The Center for X-Ray Optics Homepage, 1995 – 2010, Filter transmissions,  
239 [https://henke.lbl.gov/optical\\_constants/filter2.html](https://henke.lbl.gov/optical_constants/filter2.html)
- 240 [13] Glenn F. Knoll. Radiation detection and measurement, 4-th ed., p. 12: DEAD TIME
- 241 [14] XIA Company Homepage, 2021, High Performance Digital Pulse Processor with mapping features,  
242 [https://xia.com/dxp\\_mercury.html](https://xia.com/dxp_mercury.html)
- 243 [15] N. Pablant et al., 41st EPS Conference on Plasma Physics (2014), Vol. 38F, P1.076.2 N.
- 244 [16] A. Pablant et al. 2012 Rev. Sci. Instrum. **83** 083506